Exosomes Secreted Under Hypoxia Enhance Invasiveness and Stemness of Prostate Cancer Cells by Targeting Adherens Junction Molecules

Anand Ramteke,[1,2] Harold Ting,[1] Chapla Agarwal,[1,3] Samiha Mateen,[1] Ranganathan Somasagara,[1] Anowar Hussain,[2] Michael Graner,[4] Barbara Frederick,[3,5] Rajesh Agarwal,[1,3] and Gagan Deep[1,3]*

[1]*Department of Pharmaceutical Sciences, Skaggs School of Pharmacy and Pharmaceutical Sciences, University of Colorado Denver, Aurora, Colorado*
[2]*Department of Molecular Biology and Biotechnology, Tezpur University, Tezpur, India*
[3]*University of Colorado Cancer Center, Aurora, Colorado*
[4]*Department of Neurosurgery, University of Colorado Denver, Aurora, Colorado*
[5]*Department of Radiation Oncology Anschutz Medical Campus, Aurora, Colorado*

Hypoxic conditions in prostate cancer (PCA) are associated with poor prognosis; however, precise mechanism/s through which hypoxia promotes malignant phenotype remains unclear. Here, we analyzed the role of exosomes from hypoxic PCA cells in enhancing the invasiveness and stemness of naïve PCA cells, as well as in promoting cancer-associated fibroblast (CAF) phenotype in prostate stromal cells (PrSC). Human PCA LNCaP and PC3 cells were exposed to hypoxic (1% O_2) or normoxic (21% O_2) conditions, and exosomes secreted under hypoxic ($Exo^{Hypoxic}$) and normoxic ($Exo^{Normoxic}$) conditions were isolated from conditioned media. Nanoparticle tracking analysis revealed that $Exo^{Hypoxic}$ have smaller average size as compared to $Exo^{Normoxic}$. Immunoblotting results showed a higher level of tetraspanins (CD63 and CD81), heat shock proteins (HSP90 and HSP70), and Annexin II in $Exo^{Hypoxic}$ compared to $Exo^{Normoxic}$. Co-culturing with $Exo^{Hypoxic}$ increased the invasiveness and motility of naïve LNCaP and PC3 cells, respectively. $Exo^{Hypoxic}$ also promoted prostasphere formation by both LNCaP and PC3 cells, and enhanced α-SMA (a CAF biomarker) expression in PrSC. Compared to $Exo^{Normoxic}$, $Exo^{Hypoxic}$ showed higher metalloproteinases activity and increased level of diverse signaling molecules (TGF-β2, TNF1α, IL6, TSG101, Akt, ILK1, and β-catenin). Furthermore, proteome analysis revealed a higher number of proteins in $Exo^{Hypoxic}$ (160 proteins) compared to $Exo^{Normoxic}$ (62 proteins), primarily associated with the remodeling of epithelial adherens junction pathway. Importantly, $Exo^{Hypoxic}$ targeted the expression of adherens junction proteins in naïve PC3 cells. These findings suggest that $Exo^{Hypoxic}$ are loaded with unique proteins that could enhance invasiveness, stemness, and induce microenvironment changes; thereby, promoting PCA aggressiveness.

Key words: exosomes; hypoxia; invasiveness; adherens junction; prostate cancer

INTRODUCTION

Prostate cancer (PCA) is the most common non-cutaneous malignancy and second leading cause of cancer-related deaths in American men. According to the American Cancer Society, in 2013, there will be an estimated 238 590 new cases and 29 720 deaths from PCA in the United States [1]. Patients with localized PCA have a high 5-year survival rate and a relatively low mortality to incidence ratio compared to other cancer types [2]. However, in patients with clinically detectable metastasis, median survival is reduced to only 12–15 months; therefore, metastasis is the main cause of high mortality among PCA patients [2–4]. Thus, a better understanding and targeting of the events associated with PCA growth and metastasis is warranted to lower mortality as well as to improve patient's quality of life.

Now it is clearly evident that the interaction between the tumor microenvironment and cancer cells plays a critical role in tumor growth, angiogenesis, epithelial to mesenchymal transition (EMT), and metastasis [5,6]. The tumor microenvironment consists of several distinct cell types, including tumor cells, cancer-associated fibroblasts (CAF), endothelial

Abbreviations: α-SMA, alpha-smooth muscle actin; CAF, cancer-associated fibroblast; DAPI, 4,6-diamidino-2-phenylindole; ECL, enhanced chemiluminescence; EMT, epithelial to mesenchymal transition; $Exo^{Hypoxic}$, exosomes secreted under hypoxia; $Exo^{Normoxic}$, exosomes secreted under normoxia; FBS, fetal bovine serum; HRP, horseradish peroxidase; HSP, heat shock proteins; IL6, interleukin 6; LOX, lysyl oxidase; MMP, matrix metalloproteinase; MS, mass spectrometry; NTA, nanoparticle tracking analysis; PAGE, polyacrylamide gel electrophoresis; PCA, prostate cancer; PKM2, pyruvate kinase M2; PrSC, prostate stromal cells; SCGM, stromal cell growth medium; SDS, sodium dodecyl sulfate; TGF-β2, transforming growth factor beta 2; TNF1α, tumor necrosis factor 1 alpha; TSG101, tumor susceptibility gene 101.

Grant sponsor: DOD; Grant number: W81XWh-12-1-0053; Grant sponsor: NCI RO1; Grant number: CA102514

*Correspondence to: Department of Pharmaceutical Sciences, Skaggs School of Pharmacy and Pharmaceutical Sciences, University of Colorado Denver, 12850 E. Montview Blvd, C238, Aurora, CO 80045.

Received 4 October 2013; Revised 16 November 2013; Accepted 26 November 2013

DOI 10.1002/mc.22124

Published online 17 December 2013 in Wiley Online Library (wileyonlinelibrary.com).

cells, macrophages, adipocytes, dendritic cells, natural killer cells, lymphocytes, etc. In addition, the tumor microenvironment is rich in non-cellular components such as cytokines, growth factors, hormones, and extracellular matrix. Tumor cells and microenvironment components communicate by cell–cell interaction as well as paracrine mechanisms involving growth factors, chemokines, and proteinases [5,7]. Recently, exosomes and microvesicles have been suggested as one of the key mechanisms of intercellular communication in the tumor microenvironment [8,9]. Exosomes are approximately 30–100 nm diameter membrane-enclosed vesicles derived from the endosomal system during multivesicular body formation [10]. The factors and stimuli that regulate exosomes packaging and release have not been fully characterized, although exosomes have been widely reported to mediate local and systemic cell communication through horizontal transfer of information such as microRNAs, mRNAs, and proteins [8,11,12]. In carcinogenesis, exosomes' role has been implicated in proliferation, angiogenesis, immune-suppression; and more recently, in the preparation of premetastatic niches in secondary organs [8,9]. For example, Peinado et al. [13] recently reported that exosomes from highly metastatic melanomas increase metastasis by educating the bone marrow-derived cells at distant premetastatic sites. Interestingly, this study also showed that primary tumor growth as well as metastasis of melanoma cells could be compromised by inhibiting exosomes biogenesis [13]. Therefore, it is clear that a better understanding of the contents of exosomes and the conditions affecting their release as well as the microenvironment changes induced by exosomes could be useful towards targeting both primary tumor growth and metastasis.

Hypoxia (low oxygen conditions) in prostate tumors has been associated with an aggressive phenotype and poor prognosis [14,15]. Hypoxia is known to induce genetic and proteomic changes in cancer cells and to select clones with enhanced invasiveness, drug resistance, and stemness [15–17]. However, the mechanism/s underlying hypoxia-mediated increase of metastasis remains unclear; this is because hypoxic conditions mostly prevail away from the invasive front, which is usually at the tumor margins. In the present study, we assessed whether under hypoxic conditions PCA cells could enhance the invasiveness and motility of naïve PCA cells via transferring information packaged in exosomes. We characterized hypoxic PCA exosomes and analyzed their role in the motility, invasiveness, and stemness of PCA cells. In addition, we analyzed the effect of exosomes on α-smooth muscle actin (α-SMA) expression in prostate fibroblasts. α-SMA is an established biomarker for the cancer-associated fibroblast (CAF) phenotype, which has been associated with the promotion of EMT, stemness, and angiogenesis in PCA [18,19]. Furthermore, we identified the unique set of proteins that are loaded in hypoxic PCA exosomes and could be responsible for the enhanced invasiveness, stemness, and microenvironment changes in PCA cells.

MATERIALS AND METHODS

Cell Lines and Reagents

Human PCA LNCaP and PC3 cells were purchased from ATCC (Manassas, VA). Human prostate stromal cells (PrSC), stromal cell growth medium (SCGM), and Bullet-kits were purchased from Lonza (Allendale, NJ). ExoQuick™, exosome-free FBS (Exo-FBS™) as well as antibodies for CD81, CD63, HSP70, and HSP90 were from System Biosciences (Mountain View, CA). Antibodies for TSG101, IL6, α-tubulin, and α-SMA were from Abcam (Cambridge, MA). TGF-β2 antibody was from Gibco (Grand Island, NY). Antibodies for TNF1α, Annexin II, β-catenin, and α-tubulin were from Santa Cruz Biotechnology (Santa Cruz, CA), and antibodies for E-cadherin, PKM2 (pyruvate kinase M2), and anti-rabbit peroxidase-conjugated secondary antibody were from Cell Signaling (Beverly, MA). DAPI was obtained from Sigma (St. Louis, MO). Enhanced chemiluminescence (ECL) detection system and anti-mouse HRP-conjugated secondary antibody were from GE Healthcare (Buckinghamshire, UK). RPMI1640 medium and other cell culture materials were from Invitrogen Corporation (Gaithersburg, MD). AccQ Tag Fluor Reagent (WAT 052880), AccQ Taq Eluent A Concentrate (WAT 052890) and AccQ Tag HPLC Column (WAT 052885) were purchased from Waters Corporation (Milford, MA). All other reagents were obtained in their commercially available highest purity grade.

Cell Culture and Hypoxia Exposure

LNCaP and PC3 cells were cultured at 37°C in a 5% CO_2 humidified environment as adherent monolayer in RPMI1640 medium supplemented with 10% fetal bovine serum (FBS) or 10% heat inactivated FBS and 100 U/mL penicillin G and 100 μg/mL streptomycin sulfate. PrSC were cultured in SCGM supplemented with Bullet-kits. For exosome isolation, LNCaP and PC3 cells were cultured in media supplemented with exosome-depleted FBS. Hypoxia experiments were performed with a Hypoxia chamber (Coy Laboratory Products, Grass Lake, Michigan) at 1% O_2 at 37°C in a 5% CO_2 humidified environment.

Exosome Isolation

Exosomes were isolated from the conditioned media following a published method [11]. LNCaP and PC3 cells were cultured for 48 h; thereafter, media was replaced with RPMI 1640 supplemented with 10% exosome-depleted FBS and cultured under normoxic (21% O_2) or hypoxic (1% O_2) conditions for 72 h. Subsequently, conditioned media was harvested and

exosomes were isolated by traditional methods using serial centrifugation at low speed, followed by ultracentrifugation (L-80 Ultracentrifuge, Beckman Coulter, Indianapolis, IN) at 30 000 rpm using type 70.1 Ti fixed angel rotor (Beckman Coulter). The exosomes were also isolated by a precipitation method using commercially available ExoQuick™ reagent (System Biosciences) according to the vendor's instructions. Briefly, conditioned media was overnight incubated with ExoQuick™ reagent, centrifuged at 5000 rpm for 2 h and the pellet was washed once with PBS, and pelleted exosomes were resuspended in PBS and stored at −20°C until further use.

Nanoparticle Tracking Analysis (NTA)

Isolated exosomes were analyzed using Nanosight LM10 system (Nanosight Ltd., Navato, CA) equipped with a blue laser (405 nm). Nanoparticles were illuminated by the laser and their movement under Brownian motion was captured for 60 s and the video recorded was subjected to NTA using the Nanosight particle tracking software to calculate nanoparticle concentrations and size distribution.

Electron Microscopy

Exosomes were suspended in glutaraldehyde, and ~3–5 μL of exosomes were applied to 400 mesh copper grids (formvar/carbon coated, glow-discharged) for 5 min, followed by negative staining with 2% uranyl acetate for 2 min. Grids were briefly washed in DI water, allowed to dry and viewed using FEI Technai Transmission electron microscope equipped with Gatan Ultrascan digital high-resolution camera.

Invasion Assay

Invasion assay was performed using matrigel coated trans-well chambers from BD Biosciences (San Jose, CA). In this assay, bottom chambers were filled with RPMI medium with 10% FBS. LNCaP cells (1×10^5) were incubated with 10 μg of LNCaP $Exo^{Normoxic}$ or $Exo^{Hypoxic}$ for 45 min in RPMI medium (with 0.5% FBS) and thereafter, seeded in the upper chambers. After 24 h of incubation under standard culture conditions, LNCaP cells on top surfaces of the membrane (noninvasive cells) were scraped with cotton swabs and cells on the bottom sides of the membrane (invasive cells) were fixed with cold methanol, stained with hematoxylin/eosin and mounted. Images were taken using Cannon Power Shot A640 camera on Zeiss inverted microscope and invasive cells were counted at 100×.

Wound Healing Assay

The effect of LNCaP $Exo^{Normoxic}$ or $Exo^{Hypoxic}$ on the motility of PC3 cells was examined in well-established wound healing assay [20]. Briefly, PC3 cells were grown to full confluency in six-well plates and wounded by pipette tips and washed twice with media to remove detached cells. Photomicrographs of initial wounds were taken using Canon Power Shot A640 digital camera (at 100× magnification). Thereafter, cells were incubated with LNCaP $Exo^{Normoxic}$ or $Exo^{Hypoxic}$ (20 μg each). Experiment was terminated after 6 h and photomicrographs of final wounds were taken for each group. Initial and final wound sizes were measured using AxioVision Rel.4.7 software, and difference between the two was used to determine migration distance using the formula: Initial wound size minus final wound size divided by 2.

Prostasphere Formation

Naïve LNCaP and PC3 cells (2.5×10^3 cells per well) were separately cultured in Corning ultra-low attachment plates in DMEM/F-12(Ham) medium containing supplements B27 and N2 (from Invitrogen) in the presence of $Exo^{Normoxic}$ or $Exo^{Hypoxic}$ (10 μg/day each for 3–4 days) from LNCaP and PC3 cells, respectively. Number of prostaspheres formed was counted under a microscope after 5–6 days.

Confocal Imaging

PrSC were seeded onto glass coverslips in 12-well plates and incubated for 24 h in low serum (0.5%) growth media along with 20 μg of $Exo^{Normoxic}$ or $Exo^{Hypoxic}$ from LNCaP and PC3 cells. After the treatment, media was removed and cells were fixed with formaldehyde/cold methanol and incubated overnight in primary antibody (anti α-SMA). The cells were then washed and treated with secondary Alexa-Fluor 488 conjugated antibody and DAPI nuclear stain. The coverslips containing cells were then mounted onto slides and images were taken by Nikon Confocal Microscope. Images were quantified for Alexa-Fluor 488-green color based upon the following scoring criterion: 0+ (no color), 1+ (dim color), 2+ (moderate color), 3+ (bright color), and 4+ (very bright color).

Zymogram Analyses

MMP activity was determined by Zymogram assay following vendor's instructions (Invitrogen). Briefly, LNCaP $Exo^{Normoxic}$ or $Exo^{Hypoxic}$ (10 μg each) were mixed with equal volume of tris–glycine SDS sample buffer (2×) and incubated at room temperature for 10 min, and then run on 10% zymogram (gelatin) gel. The gel was then processed by incubating in zymogram renaturing buffer for 30 min at room temperature followed by overnight incubation in zymogram developing buffer at 37°C and stained with Coomassie Blue. The areas of protease activity appeared as clear bands.

Western Blotting

The exosomes isolated by ExoQuick™ precipitation were lysed with lysis buffer (10 mmol/L Tris–HCl, pH 7.4, 150 mmol/L NaCl, 1% Triton X-100,

1 mmol/L EDTA, 1 mmol/L EGTA, 0.3 mmol/L phenylmethylsulfonyl fluoride, 0.2 mmol/L sodium orthovanadate, 0.5% NP40, and 5 units/mL aprotinin). PC3 cells subcellular fractionations (membrane, cytoplasmic, and nuclear) were prepared as per vendor's protocol (ThermoFisher Scientific, Rockford, IL). The protein concentration of lysates was estimated using Bio-Rad DC protein assay kit (Bio-Rad, Hercules, CA). Samples were subjected to SDS–PAGE on 8–16% tris–glycine gels and blotted onto nitrocellulose membranes. Membranes were probed with specific primary antibodies over-night at 4°C followed by peroxidase-conjugated appropriate secondary antibody for 1 h at room temperature, and visualized by ECL detection system. For certain proteins, membranes were also probed with appropriate secondary IR Dye-tagged antibodies and visualized using Odyssey infra-red imager (LI-COR Biosciences, Lincoln, NE). Membranes were also stripped and re-probed again for protein of interest. As needed, densitometry values were measured and presented below the bands as "fold change" compared to appropriate control after loading control normalization (if applicable).

1D SDS–PAGE and MS Analysis

The purified exosomes (50 μg) were electrophoresed on a 10% 1D SDS–PAGE and the gel was stained with Coomassie brilliant blue and cut into nine slices. Gel slices were digested using a protocol modified from Shevchenko [21]. Proteins were processed for protein identification by LC/MS/MS at Mass spec core facility at University of Colorado Denver. Protein database searches of the spectra were performed with Mascot v2.2 (Matrix Science) and results were collated and protein ID's generated and validated using Protein Scape (Bruker, Fremont, CA). There were at least two peptides per hit, and the protein subcellular localizations and functions were determined from the Ingenuity Systems software (Redwood City, CA; http://www.ingenuity.com/index.html). Pathway analysis and network constructions were assembled using the Ingenuity software.

Statistical Analysis

Statistical analysis was performed using SigmaStat 2.03 software (Jandel Scientific, San Rafael, CA). Data were analyzed using one-way ANOVA (Tukey test) and a statistically significant difference was considered at $P \leq 0.05$. Statistics used for IPA (Ingenuity Pathway Analysis) can be found at the website http://www.ingenuity.com/index.html.

RESULTS

Characterization of LNCaP $Exo^{Normoxic}$ and $Exo^{Hypoxic}$

LNCaP $Exo^{Normoxic}$ and $Exo^{Hypoxic}$ were analyzed for particle size distribution by nanoparticle tracking analysis (NTA). As shown in Figure 1 A, the average size of $Exo^{Hypoxic}$ (average size 141 nm) was smaller than $Exo^{Normoxic}$ (average size 187 nm). NTA data also revealed that total particle concentration per mL was comparable in LNCaP $Exo^{Normoxic}$ (0.26E8 particles/mL) and $Exo^{Hypoxic}$ (0.24E8 particles/mL) after normalization with respective cell numbers. At the time of conditioned media collection for the isolation of exosomes, we observed ~50% fewer LNCaP cells under hypoxic conditions (1% O_2) compared to normoxic conditions (21% O_2), which was due to slower proliferation under hypoxic conditions. Next, we characterized LNCaP $Exo^{Normoxic}$ and $Exo^{Hypoxic}$ via electron microscopy. As shown in Figure 1B, $Exo^{Normoxic}$ and $Exo^{Hypoxic}$ were bigger than 50 nm but smaller than 100 nm. The difference between NTA and electron microscopy for exosomes size could be due to the possible aggregation of exosomes in NTA analyses.

Next, we characterized LNCaP $Exo^{Normoxic}$ and $Exo^{Hypoxic}$ for the level of proteins that are usually associated with exosomes. As shown in Figure 1C, $Exo^{Hypoxic}$ showed higher levels of tetraspanins (CD81 and CD63) compared to $Exo^{Normoxic}$. Furthermore, we also observed an increased level of HSP70 and 90 as well as Annexin II but a decreased level of Alix in $Exo^{Hypoxic}$ (Figure 1C). We did not observe any expression of endoplasmic reticulum protein Calnexin, and α-tubulin level was low in $Exo^{Normoxic}$ and $Exo^{Hypoxic}$ (Figure 1C).

$Exo^{Hypoxic}$ Enhance the Invasiveness and Motility of PCA Cells

Earlier studies have shown that hypoxia enhances the invasiveness and motility of PCA cells [16,22]. Accordingly, next we compared the effect of LNCaP $Exo^{Normoxic}$ and $Exo^{Hypoxic}$ on the invasiveness of naïve LNCaP cells. As shown in Figure 2A, compared to $Exo^{Normoxic}$, co-culturing with $Exo^{Hypoxic}$ significantly increased the invasiveness of naïve LNCaP cells (approximately fourfold increase, $P \leq 0.05$). Furthermore, we compared LNCaP $Exo^{Normoxic}$ and $Exo^{Hypoxic}$ for their effect on the motility of naïve PC3 cells in a wound healing assay. We selected PC3 cells as LNCaP cells are not suitable for this assay. As shown in Figure 2B, at 0 h, the size of the wound was almost equal in all the groups. However, 6 h following incubation with or without exosomes, PC3 cells migrated and filled the wound to varying extent. The presence of $Exo^{Normoxic}$ only marginally increased the motility of PC3 cells; however, in the presence of $Exo^{Hypoxic}$ PC3 cells motility was significantly increased and wound was almost closed (Figure 2B, left panel). Distance traveled by cells in each case was also quantified, and we observed a significant increase in the cell migration distance in the presence of $Exo^{Hypoxic}$ (Figure 2B, right panel). Together, these two studies clearly established that exosomes released under hypoxia could promote the invasiveness and motility of PCA cells. This study also suggested that LNCaP $Exo^{Hypoxic}$ effect was not confined to

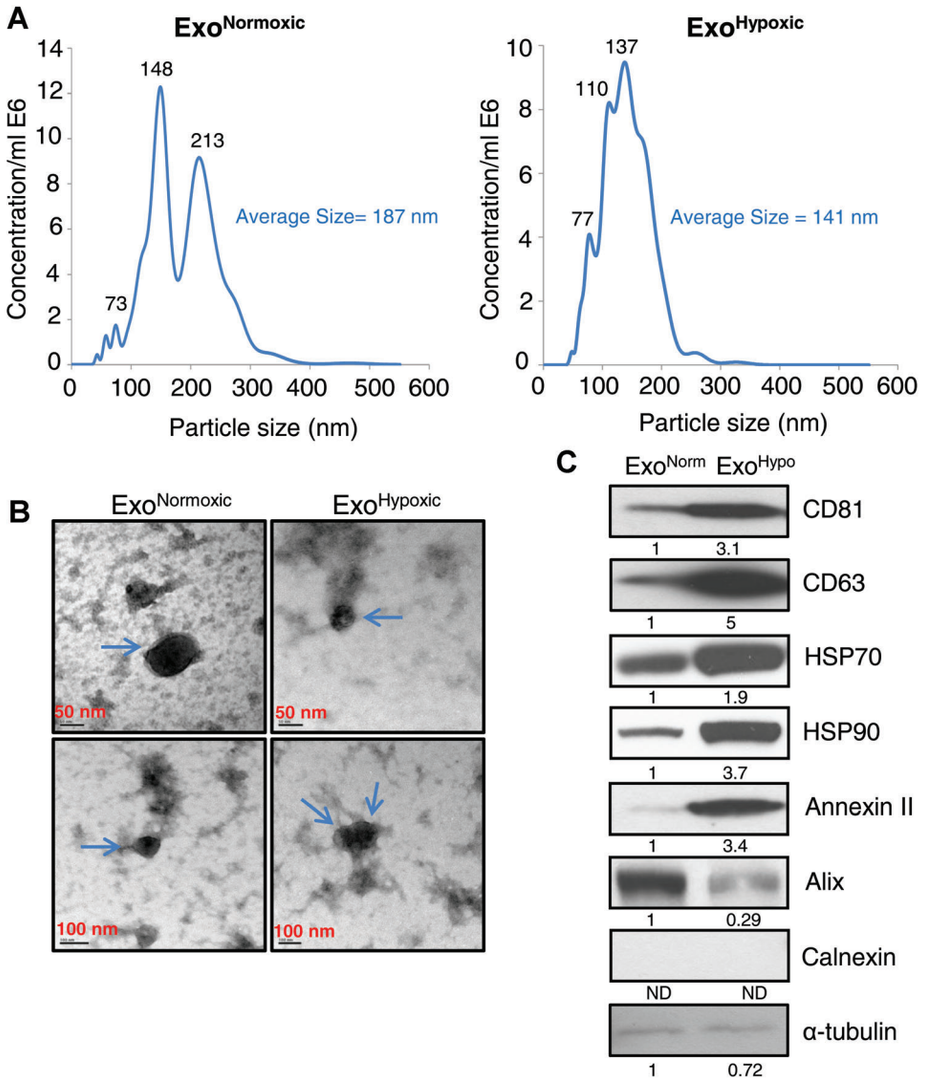

Figure 1. Characterization of Exo^{Normoxic} and Exo^{Hypoxic}. (A) Exo^{Normoxic} and Exo^{Hypoxic} were analyzed for particle size and concentration by NTA using a NanoSight device. Representative particle distributions for Exo^{Normoxic} (left panel) and Exo^{Hypoxic} (right panel) are presented. (B) Exo^{Normoxic} and Exo^{Hypoxic} were analyzed by electron microscopy as detailed in the "Materials and Methods" and representative photomicrographs are shown (arrow points to exosomes). (C) Exo^{Normoxic} and Exo^{Hypoxic} collected through precipitation method were lysed and protein expressions of CD81, CD63, HSP70, HSP90, annexin II, Alix, Calnexin, and α-tubulin were analyzed by Western blotting after equal amount of protein loading. Mean densitometry values are presented below the bands (ND: not detectable). These results were similar in at least two independent experiments.

LNCaP cells only, and LNCaP Exo^{Hypoxic} could enhance the motility of PC3 cells, a cell line not of their origin.

Exo^{Hypoxic} Enhance the Stemness of PCA Cells

Hypoxia has been associated with increased stemness in cancer cells [23]. Also, there is a great degree of overlap in cancer metastatic and stem-cell populations [24,25]. Therefore, we reasoned that besides increasing the invasiveness and motility of PCA cells, Exo^{Hypoxic} could also enhance their stemness. We analyzed the effect of Exo^{Normoxic} and Exo^{Hypoxic} on the stemness of PCA cells in a prostasphere assay, which is considered a standard in vitro assay to measure the stemness of PCA cells [26,27]. Repeated treatment with LNCaP Exo^{Hypoxic} enhanced prostaspheres number (1.5-fold increase compared to Exo^{Normoxic}, $P \leq 0.05$) in naïve LNCaP cells (Figure 3A, upper panel). Similarly, PC3 Exo^{Hypoxic} enhanced the prostaspheres number (1.9-fold increase compared to Exo^{Normoxic}, $P \leq 0.001$) in naïve PC3 cells (Figure 3A, bottom panel). Together, these

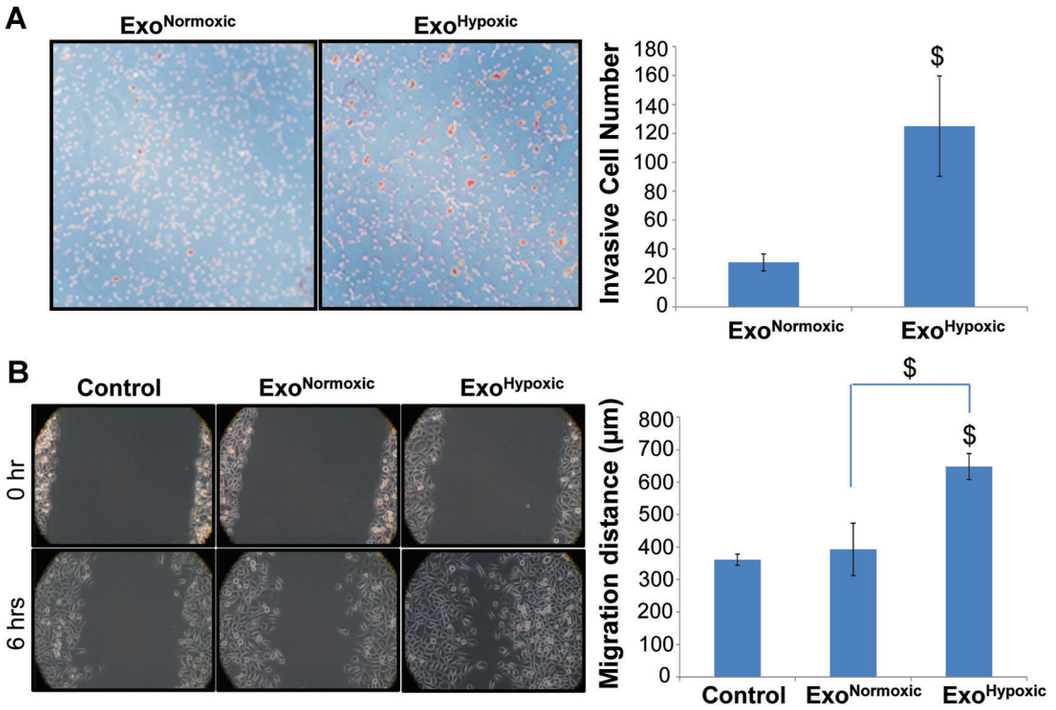

Figure 2. $Exo^{Hypoxic}$ promote invasiveness and motility in PCA cells. (A) Effects of LNCaP $Exo^{Normoxic}$ and $Exo^{Hypoxic}$ were analyzed on the invasiveness of naïve LNCaP cells using invasion chambers. Cell invasion data shown are means ± SEM of four samples. (B) Effects of LNCaP $Exo^{Normoxic}$ and $Exo^{Hypoxic}$ were analyzed on the migratory potential of PC3 cells through wound healing assays. Representative photomicrographs of initial (at 0 h) and final wounds (after 6 h) are shown at 100× magnification. Cell migration distance data shown is mean ± SEM of three samples. $^{\$}P \leq 0.05$.

results suggested that $Exo^{Hypoxic}$ could enhance the stemness of PCA cells.

$Exo^{Hypoxic}$ Enhance CAF-Type Phenotype in Prostate Fibroblasts

Cancer cells secrete several growth factors and cytokines to modify fibroblasts to a CAF-type phenotype, which is known to promote angiogenesis, stemness, and metastasis [5,18,19]. Since PCA exosomes secreted under hypoxic conditions could also affect the transformation of fibroblasts in the tumor microenvironment, we next examined the effect of $Exo^{Normoxic}$ and $Exo^{Hypoxic}$ on CAF-type phenotype induction in human PrSC. As shown in Figure 3B, basal α-SMA (a biomarker for the CAF phenotype) expression in PrSC was low, and in the presence of LNCaP and PC3 $Exo^{Normoxic}$, α-SMA expression was slightly enhanced. However, α-SMA expression was significantly higher and organized in PrSC in the presence of $Exo^{Hypoxic}$ from both LNCaP and PC3 cells (Figure 3B). TGF-β2 is a known inducer of CAF phenotype [28]; therefore TGF-β2-induced PrSC (with higher expression and well organized α-SMA) were considered as a positive control in this experiment.

$Exo^{Hypoxic}$ Possess Higher Metalloproteinase Activity and Higher Level of Key Signaling Molecules

Metalloproteinases (MMPs) have been associated with angiogenesis, metastasis, and hormone-refractory progression of PCA [29]. Hypoxia has been reported to enhance MMP-2 activity in PCA cells thereby increasing their invasiveness [16]; however, MMPs activity in hypoxic PCA exosomes has not been studied. We next compared $Exo^{Normoxic}$ and $Exo^{Hypoxic}$ for their MMPs activity in zymogram assays and as shown in Figure 4A, $Exo^{Hypoxic}$ showed higher MMP-2 and MMP-9 activity compared to $Exo^{Normoxic}$.

We next compared the $Exo^{Normoxic}$ and $Exo^{Hypoxic}$ for levels of various cytokines, growth factors, and signaling molecules that play important role in intercellular communication in the tumor microenvironment as well as PCA growth and progression [9,19,30]. As shown Figure 4B, $Exo^{Hypoxic}$ showed significantly higher levels of TGF-β2, TNF1α and IL6 compared to $Exo^{Normoxic}$. We also observed an increase in the level of Tumor Susceptibility Gene 101 (TSG101), a protein that plays a critical role in endosomal sorting and trafficking. We also detected

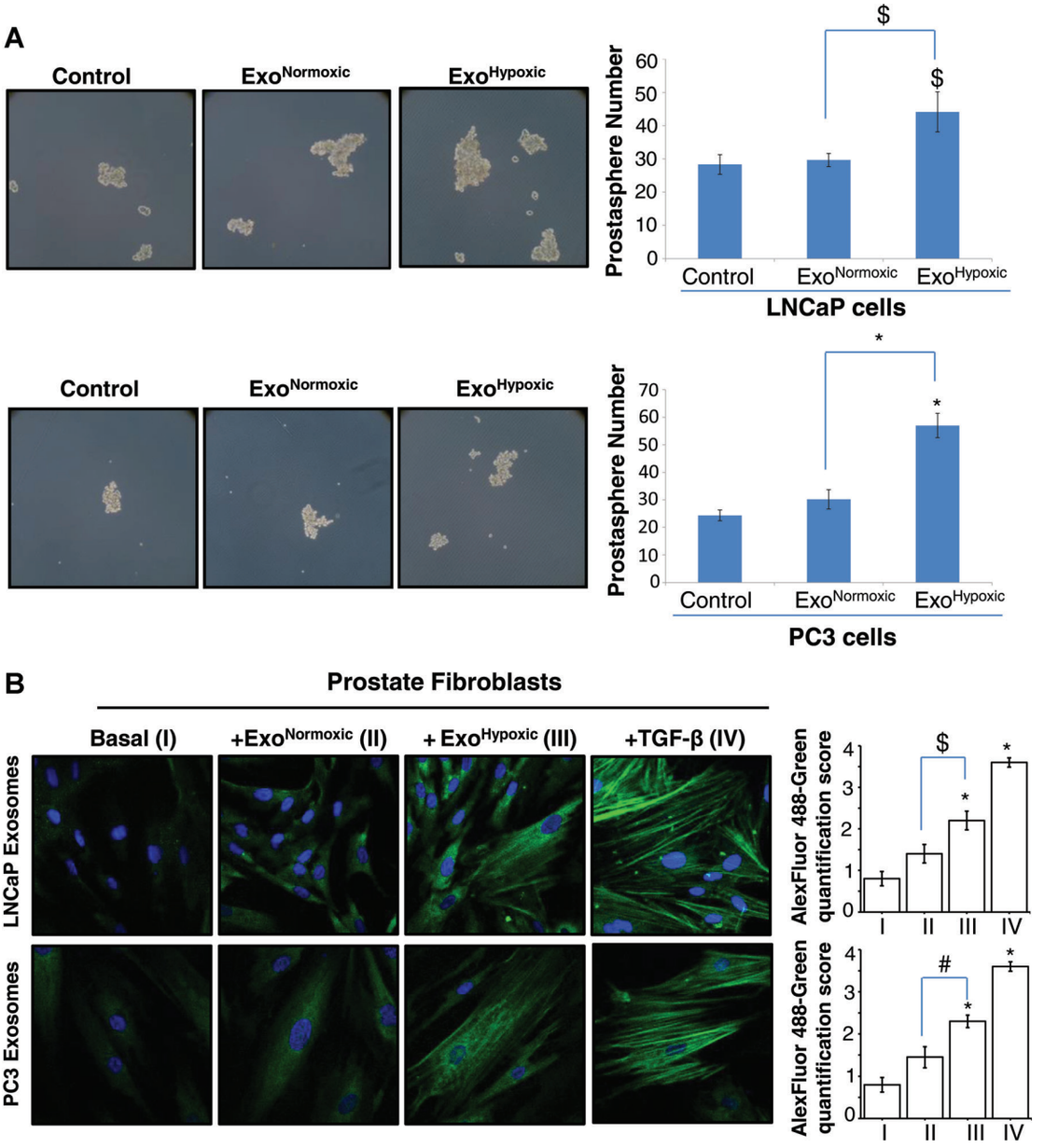

Figure 3. Exo^{Hypoxic} promote stemness in PCA cells and CAF-phenotype in prostate fibroblasts. (A) Effects of Exo^{Normoxic} and Exo^{Hypoxic} were analyzed on the stemness of naïve LNCaP (upper panel) and PC3 cells (bottom panel) following procedures detailed in the "Materials and Methods." Prostasphere formation was analyzed after 5–6 days and representative pictures are shown at 100× magnification. Prostasphere data shown is mean ± SEM of six samples. (B) Human prostate stromal cells (PrSC) were cultured in the presence of Exo^{Normoxic} and Exo^{Hypoxic} from LNCaP (upper panel) and PC3 cells (bottom panel), and α-SMA expression was analyzed by confocal microscopy. Representative images from three independent experiments are shown at 1000× magnification, where Alexa Fluor 488-green is for α-SMA while DAPI-blue stains nuclei. PrSC without exosomes represent the basal expression of α-SMA, while PrSC treated with TGF-β2 served as a positive control. Alexa-Fluor 488-green quantification data shown is mean ± SEM of twenty images from three independent experiments. $^{\$}P \leq 0.05$; $^{\#}P \leq 0.01$; $^{*}P \leq 0.001$.

higher Akt, integrin-linked kinase (ILK1), and β-catenin levels in Exo^{Hypoxic} compared to Exo^{Normoxic}, while no difference was observed in PKM2 level. These results suggest higher amounts of cytokines and signaling molecules in Exo^{Hypoxic} compared to Exo^{Normoxic}.

Exo^{Hypoxic} are Loaded With Higher Number of Proteins Associated With Distinct Signaling Pathways

Next, we performed gel-based separation of Exo^{Normoxic} and Exo^{Hypoxic} proteins with in situ protease digestion of gel slices to obtain peptides

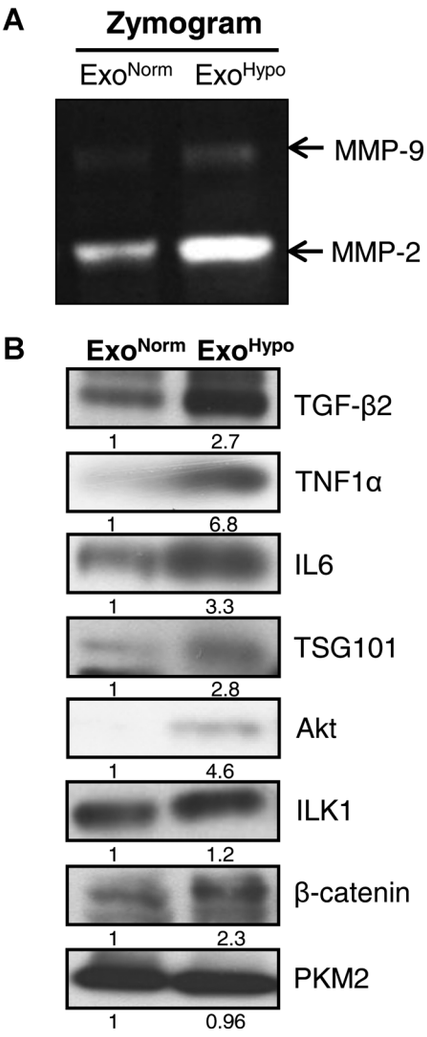

Figure 4. Exo^{Hypoxic} exhibit enhanced metalloproteinases (MMPs) activity and expression of signaling molecules. (A) MMP2 and 9 activities in Exo^{Normoxic} and Exo^{Hypoxic} were analyzed by zymogram assay. Gels were scanned and representative pictures are shown. (B) Exo^{Normoxic} and Exo^{Hypoxic} collected through precipitation method were lysed and protein expression of TGF-β2, TNF1α, IL6, TSG101, Akt, ILK1, β-catenin, and PKM2 was analyzed by Western blotting. Mean densitometry values are presented below the bands. These results were similar in at least two independent experiments.

for mass spectrometry mapping and de novo sequencing for protein identity. We identified 62 proteins in Exo^{Normoxic} and 160 proteins in Exo^{Hypoxic} (Figure 5A, left panel) and of those, 60 and 155 proteins were trackable in IPA software (Supplementary Tables I and II). The proteins identified were categorized for their subcellular or extracellular localization. As shown in Figure 5A, middle and right panels, Exo^{Normoxic} and Exo^{Hypoxic} were loaded with proteins primarily from the cytoplasm and extracellular space, with relatively low percentages of plasma membrane and nucleus-derived proteins. Compared to Exo^{Normoxic}, Exo^{Hypoxic} showed a greater percentage of cytosol-derived proteins and a lesser percentage of extracellular-derived proteins (Figure 5A, middle and right panels). However, it is important to mention here that numerous protein we categorized based upon IPA software have multiple localizations, particularly in tumors.

Using IPA software, the identified proteins were grouped into networks of associated functions and canonical pathways. In Figure 5B, we have presented the differences in the top 15 canonical pathways of Exo^{Normoxic} and Exo^{Hypoxic} associated proteins. The scores (−log [*P*-value]) reflect the probabilities of such association occurring by chance, with the threshold value for significance set at 1.25. Furthermore, the top 5 networks/associated functions for Exo^{Normoxic} proteins were "Dermatological Diseases and Conditions, Developmental Disorder, Hereditary Disorder" (Score = 65); Hair and Skin Development and Function, Dermatological Diseases and Conditions, "Respiratory Disease" (Score = 26); "Cell Death and Survival, Cardiovascular System Development and Function, Cardiovascular Disease" (Score = 20); "Lipid Metabolism, Small Molecular Biochemistry, Cellular Movement" (Score = 10); and "Cardiovascular Disease, Hematological Disease, Neurological Disease" (Score = 6). The top 5 networks/associated functions for Exo^{Hypoxic} proteins were "Protein Synthesis, Gene Expression, Cell Morphology" (Score = 55); "Cancer, Hematological Disease, Immunological Disease" (Score = 52); "Tissue Morphology, Dermatological Diseases and Conditions, Infectious Disease" (Score = 51); "Neurological Disease, Psychological Disorders, Skeletal and Muscular Disorders" (Score = 42); "Cancer, Reproductive System Disease, Cellular Assembly and Organization" (Score = 23). Figure 5C and D show the "interactome" of the highest-scoring local connecting network and functional associations within these networks for Exo^{Normoxic} and Exo^{Hypoxic}, respectively. Proteins identified in the proteomics screen are shown in black font with yellow highlights; while proteins not in the proteomics screen are shown in blue color (Figure 5C and D). Direct interactions between identified proteins are indicated by solid lines and indirect connections are shown with broken lines. Figure 5C demonstrates the strong connectivity of the chaperone and cytoskeletal protein system with transcriptional regulators (CAND1, EEFs, and ILF2) and kinases (Akt and PGK1) in Exo^{Normoxic}. Similarly, Figure 5D demonstrates the strong connectivity of the chaperone and cytoskeletal protein system with transcriptional regulators (CAND1, EEFs, and HNRNPD) and kinases (JNK and CKB) in Exo^{Hypoxic}.

Exo^{Hypoxic} Target Adherens Junction Molecules in PCA Cells

Mass spectrometry results suggested that the proteins in Exo^{Hypoxic} are associated with the remodeling of the epithelial adherens junction and cytoskeleton signaling (Figure 5B). Therefore, we

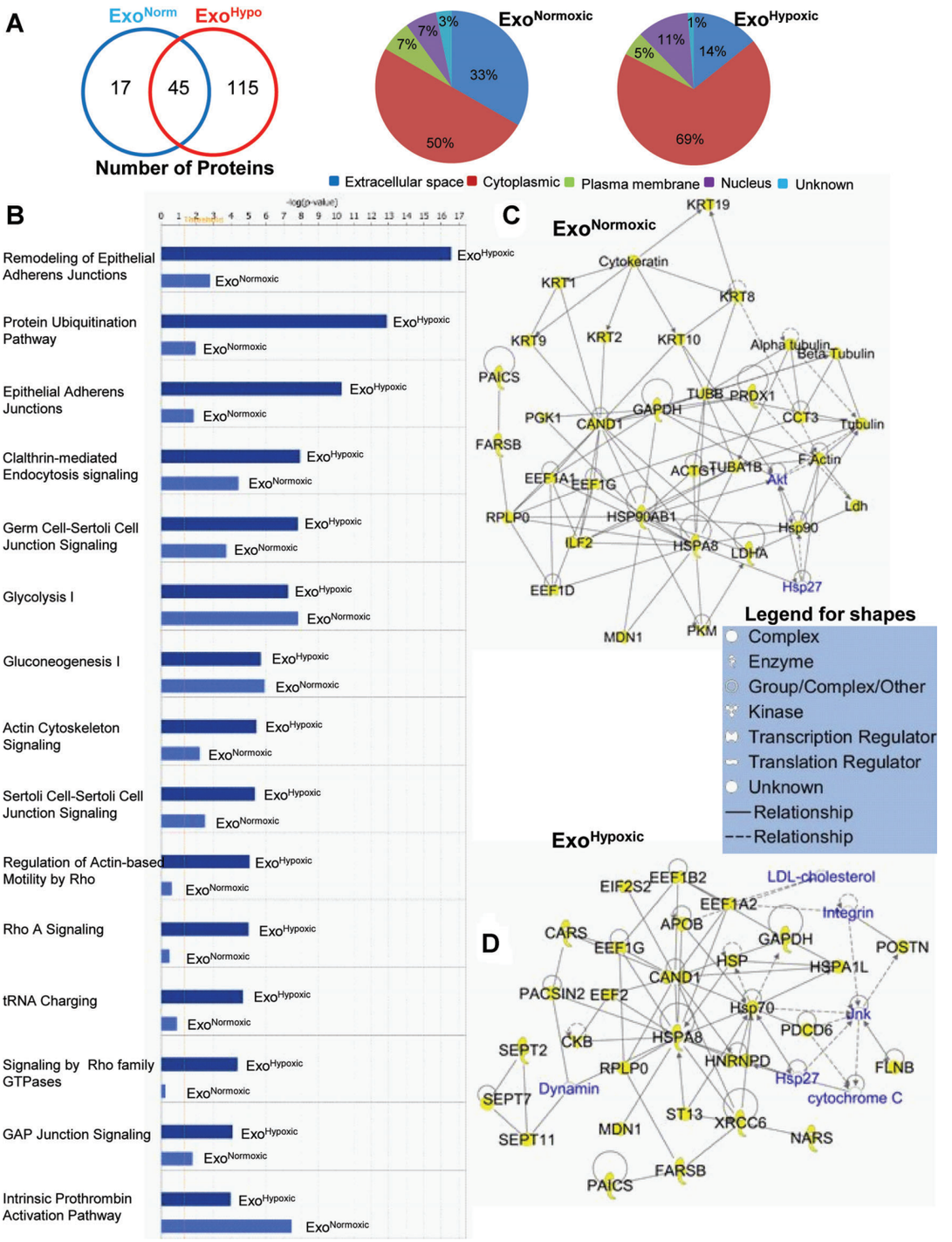

Figure 5. Characterization of Exo^{Normoxic} and Exo^{Hypoxic} proteins by mass spectrometry. (A) Total proteins (both distinct and overlapping) present in Exo^{Normoxic} and Exo^{Hypoxic} are presented in a Venn diagram (left panel). Proteins were characterized using Ingenuity IPA software, and proteins subcellular (or extracellular) localization is presented in pie diagrams (middle and right panel). (B) Exo^{Normoxic} and Exo^{Hypoxic} total protein data were compared using Ingenuity IPA software. Comparisons of the top 15 canonical pathways are shown. Scores (total number of proteins in the sample vs. total number of known proteins of that pathway) are plotted as −log value, which is derived from a *P*-value and indicates the likelihood of the Focus Proteins in a network being found together due to random chance. Threshold value is set at 1.25. (C and D) Exo^{Normoxic} and Exo^{Hypoxic} proteins clustered within the top networks/associated functions as derived from IPA algorithms are shown as members of the "interactomes." Protein shapes are indicative of function and that legend is shown.

examined the effect of LNCaP $Exo^{Hypoxic}$ on the adherens junction proteins in naïve PC3 cells. It is important to mention here that adherens junction proteins at the membrane (E-cadherin and catenins) maintain cell–cell contact and inhibit invasiveness/motility of cells. Our results showed that compared to $Exo^{Normoxic}$, $Exo^{Hypoxic}$ treatment decreased E-cadherin expression in the membrane fraction of PC3 cells (Figure 6A). We did not observe E-cadherin expression in the cytoplasmic fraction confirming the purity of membrane fractions. Furthermore, there was an increase in the nuclear and cytoplasmic β-catenin level in PC3 cells in the presence of $Exo^{Hypoxic}$ compared to $Exo^{Normoxic}$ but there was no significant change in the β-catenin level in the membrane fraction. PARP and α-tubulin blots confirmed equal protein loading in nuclear and cytoplasmic fractions, respectively.

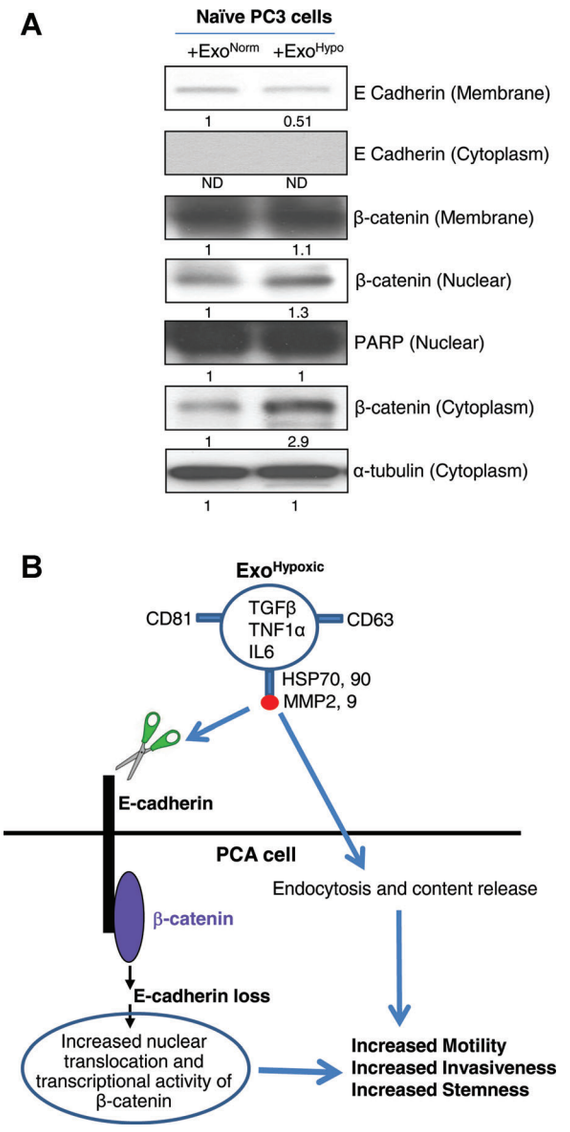

Figure 6. $Exo^{Hypoxic}$ target adherens junction proteins in PC3 cells. (A) Naïve PC3 cells were cultured for 24 h in 0.5% FBS condition, and thereafter treated with LNCaP $Exo^{Normoxic}$ and $Exo^{Hypoxic}$ (100 μg/day each) for 3 days. Thereafter, expression of adherens junction molecules E-cadherin and β-catenin was analyzed in various subcellular fractions. PARP and α-tubulin blots are presented as loading control for nuclear and cytoplasmic fractions, respectively. Mean densitometry values are presented below the bands. ND: not detectable (B) Proposed mechanism for increased motility, invasiveness, and stemness of PCA cells by exosomes secreted under hypoxic conditions. $Exo^{Hypoxic}$ could disrupt adherens junctions by promoting E-cadherin degradation as well as nuclear translocation of β-catenin, thereby enhancing the motility, invasiveness, and stemness of PCA cells.

DISCUSSION

As the primary tumor mass grows, tumor cells at the core get limited supply of oxygen and nutrients and are immersed in a stew of metabolic waste, acidic pH and necrotic cells, a physiological condition termed as "hypoxia." To overcome these hostile conditions, tumor cells activate transcriptional machinery leading to neo-angiogenesis, altered anaerobic metabolism and increased invasiveness [15,23]. However, the precise mechanism through which hypoxic tumor cells at the core of a tumor transmit signals to cells at the periphery ("the invasive front") for migration remains unknown. We hypothesized that hypoxic prostate tumor cells secrete "exosomes," small vesicles of approximately 30–100 nM diameter carrying proteins, mRNA and miRNAs, which fuse with the surrounding and/or distant tumor cells and microenvironment cells (such as fibroblasts) and significantly enhance PCA cells invasiveness and metastasis. Results from present study support this hypothesis, and for the first time we present that (1) exosomes secreted by PCA cells under hypoxia are loaded with significantly higher number of proteins; (2) hypoxic PCA exosomes could target adherens junction molecules; and (3) hypoxic PCA exosomes could significantly enhance the motility, invasiveness, and stemness of naïve PCA cells.

Recent studies suggested that hypoxic conditions could promote metastasis through remodeling and preparing distant premetastatic niches [31–33]. In this regard, Erler et al. [31] reported that lysyl oxidase (LOX) secreted by hypoxic breast tumor cells plays an important role in the enhancement of metastatic tumor growth through promoting the recruitment of bone marrow cells at premetastatic niches. Similarly, Wong et al. [32] reported that HIF-1α is a critical regulator of breast cancer metastatic niche formation through the induction of LOX family members. Hypoxic conditions also promote the release of exosomes by breast cancer cells in a HIF-1α dependent manner [34]. Thus, there is a strong possibility that under hypoxic conditions, signals for enhanced invasiveness are transferred through exosomes both locally as well as to distant premetastatic niches. Peinado et al. [13] recently confirmed that exosomes play an important role in premetastatic niches

formation even though this study did not analyze the hypoxia status of the primary melanoma tumors. Results from the present study showed a higher number of proteins loaded in hypoxic exosomes even though we did not observe any additional increases in exosomes number under hypoxic conditions. Importantly, several of the $Exo^{Hypoxic}$ proteins (e.g., TGF-β, IL6, TNF1α, MMPs, etc.) have been implicated in promoting premetastatic niche formation as well as inducing stemness and EMT in cancer cells [9,19,23,30].

It is known that metastasis by PCA cells involves multiple steps, and among these events, EMT has for some time been considered an absolute and indispensable element for metastasis [35,36]. During EMT, cancer cells shed their epithelial characteristics, detach from epithelial sheets and undergo cytoskeletal alterations towards a more "mesenchymal phenotype" and acquire a high degree of motility and invasiveness [35,36]. The molecular basis of EMT is very complex and involves several interconnected pathways that down-regulate the expression of adherens junction molecule E-cadherin, which is well known for regulating cell-to-cell contact, cell shape and polarity [35,37]. E-cadherin connects adjacent cells through homophilic interactions and is also linked to the cytoskeleton though multicatenin complex attached to their cytoplasmic tails [38,39]. In this complex, β-catenin and p120 are directly associated with E-cadherin, while α-catenin is the link between β-catenin and the actin microfilament network of the cytoskeleton [38,39]. Loss of E-cadherin results in loss of cell to cell contact, disruption of E-cadherin–catenin complex, abnormal activation of β-catenin signaling and cellular cytoskeletal alterations [35,40]. Overall, these changes are essential for cells to lose their epithelial polarity and to acquire an invasive phenotype [35,36]. In primary PCA, reduced E-cadherin expression and nuclear β-catenin expression have been correlated with increased tumor grade, metastasis, and a poor prognosis [41–43]. Interestingly, Gupta et al. [44] have shown in breast cancer cells that E-cadherin down-regulation not only induces EMT and invasiveness but also promotes cancer stem cell population. In the present study, MS and IPA analyses showed that $Exo^{Hypoxic}$ proteins are strongly involved in canonical pathways linked with epithelial adherens junctions and cytoskeleton remodeling. Furthermore, we observed that $Exo^{Hypoxic}$ promoted E-cadherin loss in PC3 cells along with an increase in cytoplasmic and nuclear β-catenin expression. Based upon known literature, these changes could be responsible for the observed increase in the invasiveness, motility, and stemness of PCA cells by $Exo^{Hypoxic}$; however, we did not analyze the mechanisms through which $Exo^{Hypoxic}$ targets elements of the adherens junction, whether it is through the MMP-mediated cleavage of E-cadherin or through the protein and miRNA content released by $Exo^{Hypoxic}$ in naïve PCA cells (as shown in the model described in Figure 6B).

Overall, the present study provides new evidence that under hypoxic conditions, the aggressiveness of PCA cells could be increased through exosomes. Further studies are warranted to confirm these results in in vivo settings, and to understand the role of specific proteins and miRNAs loaded in hypoxic exosomes. Also, we need to better understand the alterations in exosome production and release machinery under hypoxic conditions, which would be helpful to target the production of exosomes and to prevent metastatic onset in PCA cells.

ACKNOWLEDGMENTS

Authors acknowledge the Mass Spec Core Facility at Skaggs School of Pharmacy and Pharmaceutical Sciences, University of Colorado Denver. Authors are also thankful to Department of Biotechnology (DBT), Government of India for providing Overseas Associateship to Dr. Anand Ramteke. This work was supported by DOD award # W81XWh-12-1-0053 (to G.D.) and NCI RO1 grant CA102514 (to R.A.).

REFERENCES

1. Siegel R, Naishadham D, Jemal A. Cancer statistics, 2013. CA Cancer J Clin 2013;63:11–30.
2. Kingsley LA, Fournier PG, Chirgwin JM, Guise TA. Molecular biology of bone metastasis. Mol Cancer Ther 2007;6:2609–2617.
3. Tantivejkul K, Kalikin LM, Pienta KJ. Dynamic process of prostate cancer metastasis to bone. J Cell Biochem 2004; 91:706–717.
4. Hadaschik BA, Gleave ME. Therapeutic options for hormone-refractory prostate cancer in 2007. Urol Oncol 2007;25:413–419.
5. Albini A, Sporn MB. The tumour microenvironment as a target for chemoprevention. Nat Rev Cancer 2007;7:139–147.
6. Joyce JA. Therapeutic targeting of the tumor microenvironment. Cancer Cell 2005;7:513–520.
7. Deep G, Agarwal R. Targeting tumor micro environment with silibinin: Promise and potential for a translational cancer chemopreventive strategy. Curr Cancer Drug Targets 2013;13: 486–499.
8. Azmi AS, Bao B, Sarkar FH. Exosomes in cancer development, metastasis, and drug resistance: A comprehensive review. Cancer Metastasis Rev 2013;32:623–642.
9. Sceneay J, Smyth MJ, Moller A. The pre-metastatic niche: Finding common ground. Cancer Metastasis Rev 2013;32: 449–464.
10. Keller S, Sanderson MP, Stoeck A, Altevogt P. Exosomes: From biogenesis and secretion to biological function. Immunol Lett 2006;107:102–108.
11. Epple LM, Griffiths SG, Dechkovskaia AM, et al. Medulloblastoma exosome proteomics yield functional roles for extracellular vesicles. PLoS ONE 2012;7:e42064.
12. Hosseini-Beheshti E, Pham S, Adomat H, Li N, Tomlinson Guns ES. Exosomes as biomarker enriched microvesicles: Characterization of exosomal proteins derived from a panel of prostate cell lines with distinct AR phenotypes. Mol Cell Proteomics 2012;11:863–885.
13. Peinado H, Aleckovic M, Lavotshkin S, et al. Melanoma exosomes educate bone marrow progenitor cells toward a pro-metastatic phenotype through MET. Nat Med 2012;18: 883–891.

14. Bao B, Ahmad A, Kong D, et al. Hypoxia induced aggressiveness of prostate cancer cells is linked with deregulated expression of VEGF, IL-6 and miRNAs that are attenuated by CDF. PLoS ONE 2012;7:e43726.
15. Tatum JL, Kelloff GJ, Gillies RJ, et al. Hypoxia: Importance in tumor biology, noninvasive measurement by imaging, and value of its measurement in the management of cancer therapy. Int J Radiat Biol 2006;82:699–757.
16. Dai Y, Bae K, Siemann DW. Impact of hypoxia on the metastatic potential of human prostate cancer cells. Int J Radiat Oncol Biol Phys 2011;81:521–528.
17. Butterworth KT, McCarthy HO, Devlin A, et al. Hypoxia selects for androgen independent LNCaP cells with a more malignant geno- and phenotype. Int J Cancer 2008;123:760–768.
18. Fiaschi T, Giannoni E, Taddei ML, et al. Carbonic anhydrase IX from cancer-associated fibroblasts drives epithelial–mesenchymal transition in prostate carcinoma cells. Cell Cycle 2013;12:1791–1801.
19. Giannoni E, Bianchini F, Masieri L, et al. Reciprocal activation of prostate cancer cells and cancer-associated fibroblasts stimulates epithelial–mesenchymal transition and cancer stemness. Cancer Res 2010;70:6945–6956.
20. Deep G, Gangar SC, Agarwal C, Agarwal R. Role of E-cadherin in antimigratory and antiinvasive efficacy of silibinin in prostate cancer cells. Cancer Prev Res (Phila) 2011;4:1222–1232.
21. Shevchenko A. Evaluation of the efficiency of in-gel digestion of proteins by peptide isotopic labeling and MALDI mass spectrometry. Anal Biochem 2001;296:279–283.
22. Luo Y, He DL, Ning L, et al. Hypoxia-inducible factor-1 alpha induces the epithelial–mesenchymal transition of human prostatecancer cells. Chin Med J 2006;119:713–718.
23. Mimeault M, Batra SK. Hypoxia-inducing factors as master regulators of stemness properties and altered metabolism of cancer- and metastasis-initiating cells. J Cell Mol Med 2013;17:30–54.
24. Mani SA, Guo W, Liao MJ, et al. The epithelial–mesenchymal transition generates cells with properties of stem cells. Cell 2008;133:704–715.
25. Polyak K, Weinberg RA. Transitions between epithelial and mesenchymal states: Acquisition of malignant and stem cell traits. Nat Rev Cancer 2009;9:265–273.
26. Bisson I, Prowse DM. WNT signaling regulates self-renewal and differentiation of prostate cancer cells with stem cell characteristics. Cell Res 2009;19:683–697.
27. Guzman-Ramirez N, Voller M, Wetterwald A, et al. In vitro propagation and characterization of neoplastic stem/progenitor-like cells from human prostate cancer tissue. Prostate 2009;69:1683–1693.
28. Kojima Y, Acar A, Eaton EN, et al. Autocrine TGF-beta and stromal cell-derived factor-1 (SDF-1) signaling drives the evolution of tumor-promoting mammary stromal myofibroblasts. Proc Natl Acad Sci USA 2010;107:20009–20014.
29. Miyamoto H, Altuwaijri S, Cai Y, Messing EM, Chang C. Inhibition of the Akt, cyclooxygenase-2, and matrix metalloproteinase-9 pathways in combination with androgen deprivation therapy: Potential therapeutic approaches for prostate cancer. Mol Carcinog 2005;44:1–10.
30. Meads MB, Hazlehurst LA, Dalton WS. The bone marrow microenvironment as a tumor sanctuary and contributor to drug resistance. Clin Cancer Res 2008;14:2519–2526.
31. Erler JT, Bennewith KL, Cox TR, et al. Hypoxia-induced lysyl oxidase is a critical mediator of bone marrow cell recruitment to form the premetastatic niche. Cancer Cell 2009;15:35–44.
32. Wong CC, Gilkes DM, Zhang H, et al. Hypoxia-inducible factor 1 is a master regulator of breast cancer metastatic niche formation. Proc Natl Acad Sci USA 2011;108:16369–16374.
33. Sceneay J, Chow MT, Chen A, et al. Primary tumor hypoxia recruits CD11b+/Ly6Cmed/Ly6G+ immune suppressor cells and compromises NK cell cytotoxicity in the premetastatic niche. Cancer Res 2012;72:3906–3911.
34. King HW, Michael MZ, Gleadle JM. Hypoxic enhancement of exosome release by breast cancer cells. BMC Cancer 2012;12:421.
35. Guarino M, Rubino B, Ballabio G. The role of epithelial–mesenchymal transition in cancer pathology. Pathology 2007;39:305–318.
36. Christiansen JJ, Rajasekaran AK. Reassessing epithelial to mesenchymal transition as a prerequisite for carcinoma invasion and metastasis. Cancer Res 2006;66:8319–8326.
37. Baranwal S, Alahari SK. Molecular mechanisms controlling E-cadherin expression in breast cancer. Biochem Biophys Res Commun 2009;384:6–11.
38. Inge LJ, Rajasekaran SA, Wolle D, et al. alpha-Catenin overrides Src-dependent activation of beta-catenin oncogenic signaling. Mol Cancer Ther 2008;7:1386–1397.
39. Ebnet K. Organization of multiprotein complexes at cell–cell junctions. Histochem Cell Biol 2008;130:1–20.
40. Onder TT, Gupta PB, Mani SA, et al. Loss of E-cadherin promotes metastasis via multiple downstream transcriptional pathways. Cancer Res 2008;68:3645–3654.
41. Umbas R, Isaacs WB, Bringuier PP, et al. Decreased E-cadherin expression is associated with poor prognosis in patients with prostate cancer. Cancer Res 1994;54:3929–3933.
42. Umbas R, Schalken JA, Aalders TW, et al. Expression of the cellular adhesion molecule E-cadherin is reduced or absent in high-grade prostate cancer. Cancer Res 1992;52:5104–5109.
43. Cheng L, Nagabhushan M, Pretlow TP, Amini SB, Pretlow TG. Expression of E-cadherin in primary and metastatic prostate cancer. Am J Pathol 1996;148:1375–1380.
44. Gupta PB, Onder TT, Jiang G, et al. Identification of selective inhibitors of cancer stem cells by high-throughput screening. Cell 2009;138:645–659.

SUPPORTING INFORMATION

Additional supporting information may be found in the online version of this article at the publisher's web-site.